

Analysis of Early-age cracking in restrained ring specimens of high performance concrete using finite element method

Dr. **Nguyen Quang Phu**, Faculty of Hydraulic Engineering of Water Resources University, Vietnam

MEng. **Do Viet Thang**, Hydraulic Construction Institute, Vietnam

Prof. **Jiang lin hua**

College of Materials Science and Engineering, Hohai University, Nanjing 210098, China

liu jiaping

Jiangsu Institute of Building Science, Nanjing 210008, China

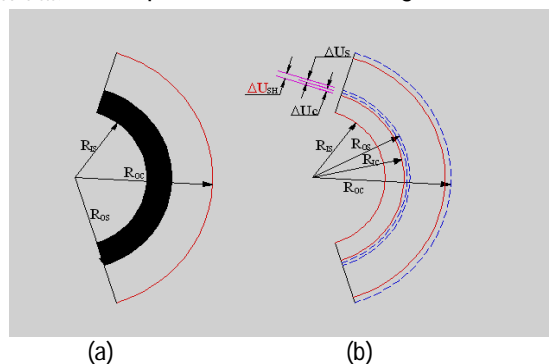
1. Introduction

High-performance concrete (HPC) was defined as concrete which always provides specific performance advantages in terms of strength and durability to compare with the conventional concrete. Recently, the use of high-performance concrete has increased. High-performance concrete mixtures are usually produced with water/binder (W/B) ratios in the range of 0.2 - 0.4, and incorporate with highly-active pozzolans such as silica fume (SF), fly ash (FA), and slag; so it cannot avoid the volume changes occur in concrete as a result of drying, self-desiccation, chemical reactions, and temperature change (ACI Committee 209)^[1]. Hence, the problems with early age cracking become prominent phenomenon. This paper used a numerical analytical study with finite element method (FEM), to predict cracking of high performance concrete in restrained ring specimens.

There were a lot of methods to determine the early age behaviour of concrete under restrained shrinkage (bar specimens, plate specimens, and ring specimens); perhaps the ring test is the most common method applied to assess early age cracking in HPC's. When the concrete exposed to dry, the shrinkage of concrete is prevented by the steel ring, as a result for the tensile stress in the concrete develop. At the first days, when the residual stress exceeded the tensile strength of the concrete that reason, the early age cracking was occurred.

The ring test method is simple in use, the fact that is limited with respect to providing quantitative information on early age stress development and the exact conditions under which cracking is taking place is referred as a disadvantage of the method. This paper is presented the finite element method (FEM) that was used in order to acquire quantitative information on early age stress development and early age cracking, using experimental data acquired from the ring test.

The restraint from the steel ring can be simulated by separating the steel and concrete ring and using a "shrink-fit" approach. The concrete ring is permitted to shrink amount (ΔU_{Sh}) that is equal to that caused by drying and autogenous shrinkage. The composite cylinder can be considered to have a fictitious pressure that is applied on the outer surface of the steel ring that is equal to the pressure on the internal surface of the concrete ring (Hossain and Weiss 2003a)^[2]. The pressure is adjusted until the steel ring is compressed (ΔU_{Steel}) and the concrete ring is expanded ($\Delta U_{concrete}$) to compensate for the shrinkage as shown in Fig 1.



(a) Before concrete shrinkage occurs

(b) Removing constraint and allowing the concrete to shrink

Figure 1. Geometry of the ring to determine the elastic response

Dally and Riley (1991)^[3] provided the solution for the radial displacement of a hollow cylinder (ring) exposed to uniform external pressure which can be used to describe the steel ring. Since the circumferential strain in the ring can be computed by dividing the radial displacement by the radius (Weiss et al. 2000)^[4], the actual residual interface pressure (p_{Residual}) can be computed as the pressure required to cause a strain that is equivalent to the measured strain in the steel ($\varepsilon_{\text{Steel}}$) as shown in Equation (1) (Weiss et al. 2000; Weiss and Furgeson 2001)^[4, 5].

$$p_{\text{Residual}}(t) = -\varepsilon_{\text{steel}}(t) \cdot E_S \cdot \frac{R_{OS}^2 - R_{IS}^2}{2R_{OS}^2} \quad (1)$$

Where: $\varepsilon_{\text{steel}}(t)$ is the strain in the steel can be obtained experimentally using strain gage on the inner surface of the steel ring;

E_S is the elastic modulus of the steel;

R_{OS} and R_{IS} are the outer and inner radius of the steel ring respectively.

The pressure that can be thought to act on the steel ring could be related to an internal fictitious pressure that acts on the concrete ring and as a result the stress distribution in the concrete ring can be determined as shown in Equation (2) and (3) (Hossain and Weiss 2003a; Timoshenko and Goodier 1987)^[2, 6].

$$\sigma_{\theta\theta, \text{rest-ring}}(r) = p_{\text{Residual}} \cdot \frac{R_{OS}^2}{R_{OC}^2 - R_{OS}^2} \left(1 + \frac{R_{OC}^2}{r^2} \right) \quad (2)$$

$$\Rightarrow \sigma_{\theta\theta, \text{rest-ring}}(r) = -\varepsilon_{\text{steel}}(t) \cdot E_S \cdot \frac{R_{OS}^2 - R_{IS}^2}{2(R_{OC}^2 - R_{OS}^2)} \left(1 + \frac{R_{OC}^2}{r^2} \right) \quad (3)$$

The elements will start cracking as the stress in a particular layer exceeds the tensile strength of concrete (f_t).

2. The ring specimens

The FEM of the ring test was performed using the software of ANSYS. The dimensions of the ring setup and the boundary conditions are shown in Fig. 2. The ring test used in this research was similar the AASHTO ring (AASHTO PP 34-98)^[7], and other researchers (Hossain A. B and Weiss J 2004)^[8] with a 75 mm thick concrete annulus was cast around a steel ring which has the steel wall thickness was 19 mm. The steel ring had 4 strain gages attached at the mid-height of the inner surface of the steel ring. Steel strain was monitored over time. The average strain information monitored by the strain gages was used as an input for the FEM.

The concrete ring was sealed surrounding circumference. The boundary conditions by permitting drying from only the top and bottom surface of the ring, moisture can only be lost along one plan. As the concrete shrinks, the steel ring was pressurized at the outer surface.

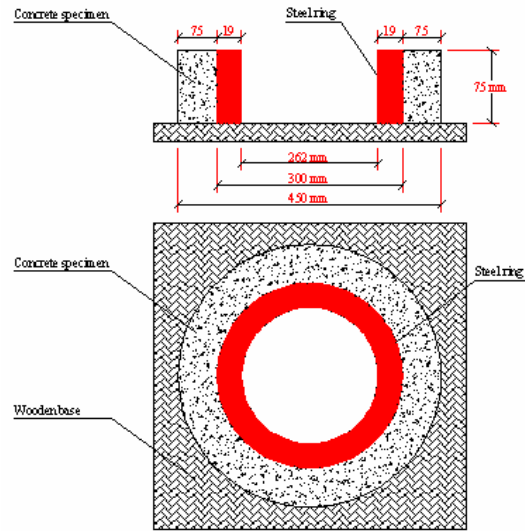


Figure 2. The geometry of ring specimen

3. Materials, concrete material properties

3.1. Materials

3.1.1. Cement

Portland cement (C) with a 42.5 grade from the Nanjing Jiangnan cement plant was used. The compressive strength of the cement (GB/T 17671-1999)^[9] was 49.7 MPa at 7 days and 60.1 MPa 28 days. The chemical composition and physical properties of the cement are presented in Table 1.

Table 1. Chemical composition and physical properties of Portland cement

Main chemical composition (%)							Density (g/cm ³)	Specific surface (m ² /kg)
SiO ₂	Al ₂ O ₃	CaO	MgO	Fe ₂ O ₃	SO ₃	Loss		
20.60	5.03	64.11	1.46	4.38	1.72	1.18	3.15	450

3.1.2. Mineral admixtures

The mineral admixtures used for concrete mixes included silica fume (SF), fly ash (FA), and slag. The chemical composition and physical properties of the mineral admixtures are shown in Table 2.

Table 2. Chemical composition and physical properties of silica fume, fly ash, and slag

Mineral admixture	Main chemical composition (%)							Density (g/cm ³)	Specific surface (m ² /kg)
	SiO ₂	Al ₂ O ₃	CaO	MgO	Fe ₂ O ₃	SO ₃	Loss		
Silica fume	93.15	0.97	1.01	0.43	0.88	0.50	1.50	2.10	24 000
Fly ash	49.39	33.36	4.92	4.13	0.85	1.96	2.49	2.20	615
Slag	33.12	11.80	1.17	34.95	10.75	0.69	1.23	2.89	439

3.1.3. Fine aggregate

Natural sand was used as fine aggregate in this study. The properties of the fine aggregate are shown in Table 3.

Table 3. Properties of fine aggregate (sand)

Bulk specific gravity of oven-dry basic (g/cm ³)	Bulk density (g/cm ³)	Absorption (%)	Fineness modulus
2.66	1.65	1.50	2.90

3.1.4. Coarse aggregate

The crushed quartzite stones used as coarse aggregate in this study were composed of size 5-10 mm stone (60%) and size 10-20 mm stone (40%). The physical properties of the coarse aggregate are shown in Table 4.

Table 4. Properties of aggregate

Bulk specific gravity of oven-dry basic (g/cm ³)	Bulk density (g/cm ³)	Absorption (%)
2.76	1.70	0.50

3.1.5. Chemical admixtures

A high-range water-reducing admixture (HRWR) was identified and evaluated in this study. Table 5 lists the properties of this admixture including their designations, brand names (trade names), chemical names, color, and specific gravity. This admixture was obtained from the Jiangsu Bote Advanced Materials Co., Ltd.

Table 5. Properties of chemical admixture

Admixture designation	Brand name	Chemical name or ingredient	Color	Specific gravity (g/cm ³)
HRWR	PCA (I)	Poly-naphthalene sulfonate	Dark brown	1.04

3.2. The concrete material properties

The concrete mixes with two different water/binder ratios (0.22 and 0.40) were tested. Three mineral admixtures were used in this study: silica fume, fly ash, and slag. The mineral admixtures contains 25% FA and 25% slag was used for the W/B = 0.40 mix, and contains 15% SF and 25% FA was used for the W/B = 0.22 mix. Mixture proportions of HPC are summarized in Table 6

Table 6. Concrete mixture proportions (by weight)

W/B	Fly ash (kg/m ³)	Silica fume (kg/m ³)	Slag (kg/m ³)	Cement (kg/m ³)	Coarse aggregate (kg/m ³)	Fine aggregate (kg/m ³)	Water (kg/m ³)	HRWR (PCA-I) (kg/m ³)
0.40	100	0	100	200	1110	740	160	2.80
0.22	155	93	0	372	1150	630	136.4	15.5

The concrete was mixed in a forced mixer. The compressive strength and splitting tensile specimens were prepared and tested using 100 mm x 100 mm x 100 mm cubic moulds in accordance with the GBJ82-85^[10]. Concrete prisms (100 mm x 100 mm x 300 mm) conforming to the ASTM C469^[11] and GB/T 50081-2002^[12] were cast to measure the elastic modulus. After 24 hours, the specimens were demolded and moist-cured at 20°C and 100% relative humidity until testing.

Because of the dynamic nature of the young cement paste so there are a lot of difficulties appear when trying to simulate the restrained concrete specimen using FEM. According to the results from the average strain information monitored by the strain gages and also compared with published data^[8], this study was decided that the numerical modeling of the ring test should be based on the material properties and experimental values of concrete at five days (after casting). The mechanical properties of the concrete at five days of age and steel used, respectively, are presented in Table 7.

Table 7. Properties of material of the concrete and steel

Material	Concrete		Steel
	W/B=0.40	W/B=0.22	
Elastic modulus, E_c , GPa	35.52	50.28	200
Compressive strength, f'_c , MPa	37.50	75.69	624
Tensile strength, f'_t , MPa	2.75	5.15	-
Poisson's ratio	0.20	0.20	0.33

The stress-strain relation of the two materials under compression was also required in the FEM. As no experimental data were available with respect to the stress-strain relation of early age concrete (namely the stress-strain plot referring to the age of few early age), it was decided that this should plotted using Thorenfeldt's analytical equation. ANSYS allows the non-linearity of materials to be defined by the user in the form of solution-dependent variables, for example strain. Namely, the CONCRETE command within ANSYS allowed the compressive stress to be paired with the plastic strain. The same solution-dependent methodology used with the concrete properties was undertaken for steel, using the command PLASTIC (although the behaviour of the steel ring was proved to be linear)

4. Modeling of the ring test

Finite element modeling of the ring specimens using ANSYS software were modeled by cubic three-dimensional as shown in Fig. 3. The elements of steel ring and concrete ring are continuous at nodes because the inner surface of concrete and outer surface of steel ring are usually with contact. When the concrete shrink, the steel ring will prevent the shrinkage of concrete so that arise the stress in concrete and steel ring. According to the test set up, the two rings are constantly in contact and as the concrete ring dies, strain gages monitor the steel ring strain. In the finite element analysis the strain information was used as input using the assumption of a constrained radial displacement of the nodes of the outer circumference of the steel ring. The average strain of the steel ring was taken equal to $-70 \mu\epsilon$ for the concrete W/B = 0.40 mix and $-100 \mu\epsilon$ for the concrete W/B = 0.22 mix respectively (experimental value corresponding to the average steel strain of the fifth day). The results of the numerical modeling of the steel ring were used as the input data for the modeling of the concrete ring, based on the assumption that the outer circumference of the steel ring was in fact the inner circumference of the concrete ring, and conditions of equal radial stress component development existed in the interface.

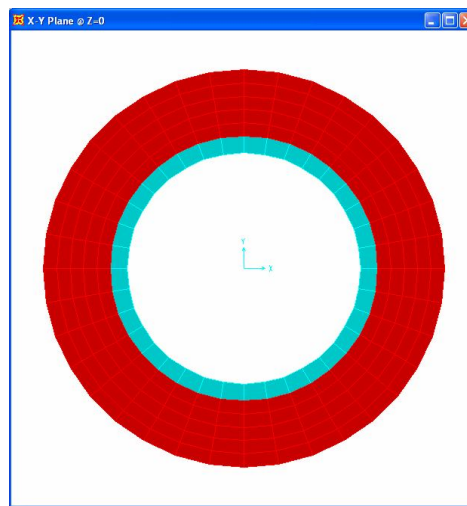


Figure 3. FEM for the analysis of the steel ring and the concrete ring specimen

5. The results and discussion

The results of the numerical modeling of the concrete ring were automatically plotted, using ANSYS post-processing. They are presented in Fig. 4. As it was generally expected stress and strain presented a uniform distribution along the ring's circumference. In discussing stresses in circular rings it is advantageous to use polar coordinates. The concrete ring subjected to a uniform radial pressure presented a uniform stress distribution along the ring's circumference, as stated in the preceding paragraph.

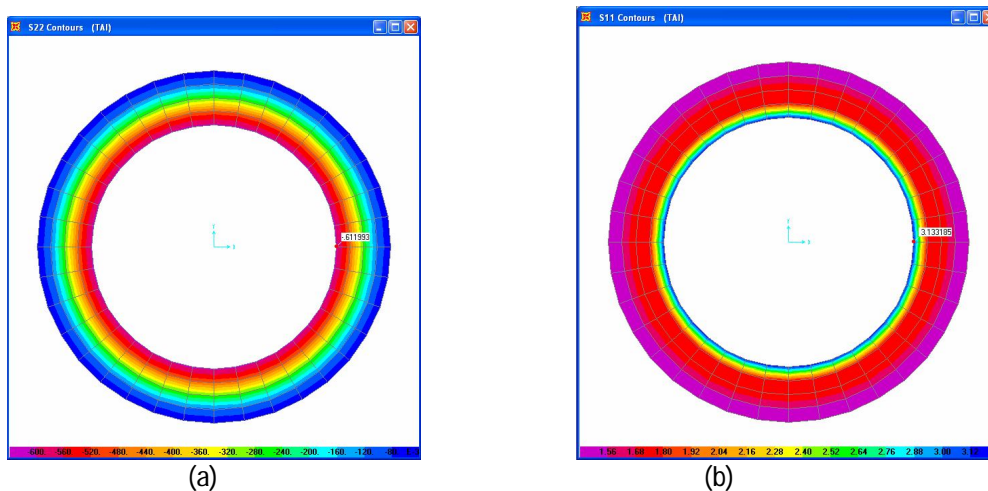


Figure 4. Stress distribution of the concrete ring: (a) in the radial direction, (b) in the circumferential direction

In Fig. 5-6 the stress developed along the concrete wall thickness were expressed in polar coordinates.

The radial, σ_r , and circumferential, σ_θ , stress produced a uniform extension in the direction of the axis of the ring. It is interesting to note that the sum $\sigma_r + \sigma_\theta$ is constant through the thickness of the wall of the ring, as theory of elasticity proposes. As expected, the maximum circumferential stress was developed at the inner circumference of the ring (at the interface between concrete and steel ring).

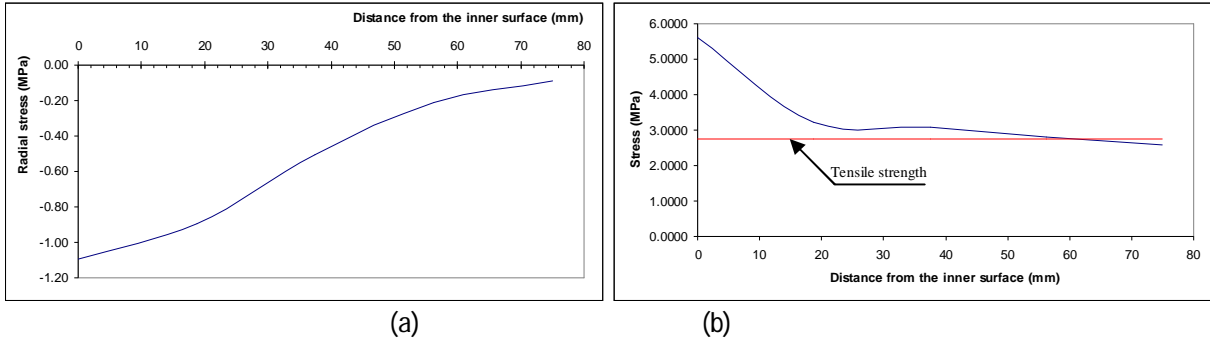


Figure 5. Variation of the stress component of concrete ring specimen: (a) in the radial direction, (b) in the circumferential direction (W/B=0.40)

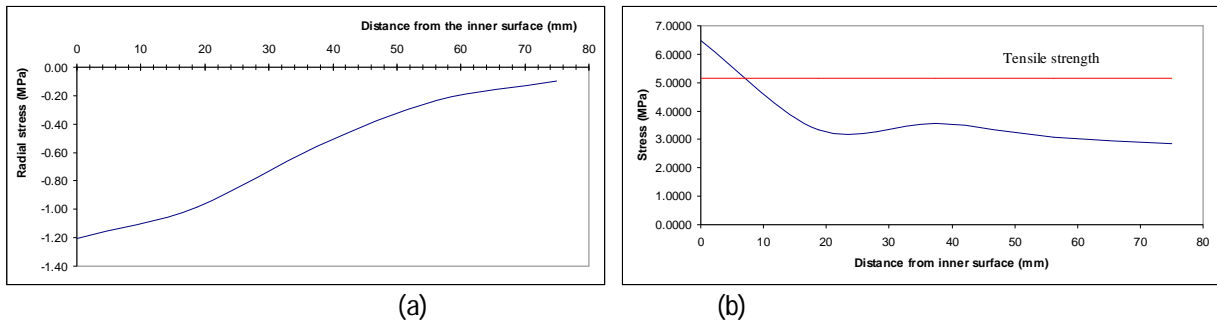


Figure 6. Variation of the stress component of concrete ring specimen: (a) in the radial direction, (b) in the circumferential direction (W/B=0.22)

As soon as the stress field of the concrete ring was estimated, appropriate failure criteria were applied, in order to predict the concrete's potential for cracking. The circumferential stress distribution along the concrete wall was compared to the concrete's tensile strength, according to the maximum circumferential strength criterion. The result is shown in Fig 5(b) and 6(b). From Fig 5(b) and 6(b) indicate that according to the criterion, the ring specimen will be cracked, after the tensile strength of concrete has been exceeded.

Taking the stress distribution along the ring's wall into consideration, it notes that the first macro-crack is expected to grow at any point along the inner circumference of the concrete ring.

6. Conclusions

The results of the average strain information monitored by the strain gages from ring test can apply to input for FEM analysis. The restrained ring test using FEM can be used to provide quantitative information on early age stress development and early age cracking of the concrete. On the other hand, the FEM procedure outlined in the preceding paragraphs could be generally used for the modeling of the behaviour of concrete under restrained shrinkage. It is also to note that the results of the FEM were in the same with experimental results of ring test carried out by the same modeling restrained ring specimens provided from strain gages monitored from data acquisition system.

From the results we can be seen that the decrease in W/B mix of concrete, the cracking is earlier and area of cracking is near the inner surface of concrete ring.

References

1. American Concrete Institute (ACI) Committee 209R-92. Prediction of Creep, Shrinkage, and Temperature Effects in Concrete Structures. ACI Manual of Concrete Practice. Farmington Hills: American Concrete Institute, 1992.
2. Hossain A. B, Weiss J. "Assessing residual stress development and stress relaxation in restrained concrete ring specimens", Cement and Concrete Composites, Vol. 25, 2003a.
3. Dal I y J. W, Riley W. F. "Experimental Stress Analysis, Third Edition", McGraw-Hill, Inc, 1991.
4. Weiss W. J, Yang W, Shah S. P. "Influence of Specimen Size and Geometry on Shrinkage Cracking", Journal of Engineering Mechanics, ASCE, 126(1), pp. 93-110, 2000.
5. Weiss W. J, Furgeson S. "Restrained Shrinkage Testing: The Impact of Specimen Geometry on Quality Control Testing for Material Performance Assessment,": Creep, Shrinkage, and Durability Mechanic of Concrete and other Quasi-Brittle Materials, ed., ULM, F. J., BAZANT, Z. P., AND WITTMAN, F. H., ELSEVIER, August 22-24 Cambridge MA, pp. 645-651, 2001.
6. Timoshenko S. P, Goodier J. N. "Theory of elasticity," McGraw-Hill Inc., 1987.
7. AASHTO PP 34, Standard practice for estimating the cracking tendency of concrete, 1998.
8. Hossain A. B, Weiss J, "Assessing Residual Stress Development and Stress Relaxation in Restrained Concrete Ring Specimens", Vol. 26, Issue 5, July 2004, pp. 531-540.
9. GB/T 17671-1999: Chinese standard, Method of Testing Cements – Determination of Strength.
10. GBJ 82-85: Chinese standard, Test Methods of Durability and Long-term Performance of Ordinary Concrete, Beijing, 1985.
11. ASTM Committee C09 on Concrete and Concrete Aggregates, ASTM C 469-02: Standard Test Method for Static Modulus of Elasticity and Poisson's Ratio of Concrete in Compression. ASTM International, United States.
12. GB/T 50081-2002: Chinese standard, Test Method of Mechanical Properties on Ordinary Concrete.